

Monoxide carbon frequency shift as a tool for the characterization of TiO₂ surfaces: Insights from first principles spectroscopy

Pablo G. Lustemberg and Damián A. Scherlis

Citation: *J. Chem. Phys.* **138**, 124702 (2013); doi: 10.1063/1.4796199

View online: <http://dx.doi.org/10.1063/1.4796199>

View Table of Contents: <http://jcp.aip.org/resource/1/JCPSA6/v138/i12>

Published by the [American Institute of Physics](#).

Additional information on J. Chem. Phys.

Journal Homepage: <http://jcp.aip.org/>

Journal Information: http://jcp.aip.org/about/about_the_journal

Top downloads: http://jcp.aip.org/features/most_downloaded

Information for Authors: <http://jcp.aip.org/authors>

ADVERTISEMENT

Instruments for advanced science

Gas Analysis



- dynamic measurement of reaction gas streams
- catalysis and thermal analysis
- molecular beam studies
- dissolved species probes
- fermentation, environmental and ecological studies

Surface Science



- UHV TPD
- SIMS
- end point detection in ion beam etch
- elemental imaging - surface mapping

Plasma Diagnostics



- plasma source characterization
- etch and deposition process
- reaction kinetic studies
- analysis of neutral and radical species

Vacuum Analysis



- partial pressure measurement and control of process gases
- reactive sputter process control
- vacuum diagnostics
- vacuum coating process monitoring

contact Hiden Analytical for further details

HIDEN
ANALYTICAL

info@hideninc.com
www.HidenAnalytical.com

CLICK to view our product catalogue



Monoxide carbon frequency shift as a tool for the characterization of TiO₂ surfaces: Insights from first principles spectroscopy

Pablo G. Lustemberg^{1,2,a)} and Damián A. Scherlis^{1,a)}

¹*Departamento de Química Inorgánica, Analítica y Química Física/INQUIMAE, Facultad de Ciencias Exactas y Naturales, Universidad de Buenos Aires, Pab II, Ciudad Universitaria, Buenos Aires C1428EHA, Argentina*

²*Instituto de Física Rosario (CONICET-UNR) and Facultad de Ciencias Exactas, Ingeniería y Agrimensura, Universidad Nacional de Rosario, Av. Pellegrini 250, Rosario S2000BTP, Argentina*

(Received 7 December 2012; accepted 7 March 2013; published online 26 March 2013)

The adsorption and vibrational frequency of CO on defective and undefective titanium dioxide surfaces is examined applying first-principles molecular dynamics simulations. In particular, the vibrational frequencies are obtained beyond the harmonic approximation, through the time correlation functions of the atomic trajectories. In agreement with experiments, at low CO coverages we find an upshift in the vibration frequency with respect to the free CO molecule, of 45 and 35 cm⁻¹ on the stoichiometric rutile (110) and anatase (101) faces, respectively. A band falling 8 cm⁻¹ below the frequency corresponding to the perfect face is observed for the reduced rutile (110) surface in the low vacancy concentration limit, where the adsorption is favored on Ti⁴⁺ sites. At a higher density of defects, adsorption on Ti³⁺ sites becomes more stable, accompanied by a downshift in the stretching band. In the case of anatase (101), we analyze the effect of subsurface oxygen vacancies, which have been shown to be predominant in this material. Interestingly, we find that the adsorption of CO on five coordinate Ti atoms placed over subsurface vacancies is favored with respect to other Ti⁴⁺ sites (7.25 against 6.95 kcal/mol), exhibiting a vibrational redshift of 20 cm⁻¹. These results provide the basis to quantitatively assess the degree of reduction of rutile and anatase surfaces via IR spectroscopy, and at the same time allow for the assignment of characteristic bands in the CO spectra on TiO₂ whose origin has remained ambiguous. © 2013 American Institute of Physics. [<http://dx.doi.org/10.1063/1.4796199>]

I. INTRODUCTION

Titanium dioxide in all possible formats and architectures—which include films, nanoparticles, and composites—has attracted the interest of materials scientists motivated by its potential uses in catalysis and photocatalysis,^{1–3} coatings,¹ optics,⁴ solar cells,^{5–7} and bioinorganic hybrid materials,⁸ among others. The morphology and the structure of the surface plays an essential role in most of these applications and its precise characterization, comprising a quantitative assessment of the exposed faces, vacancies, and other kind of defects, can be a difficult endeavor, in particular when the sample was produced via wet synthesis or other chemical processes. In this context, IR spectroscopy is a powerful technique widely applied in the case of metal oxides.⁹ The characterization of the interface structure is achieved indirectly, on the basis of the frequency shift in some vibrational mode of a small probe molecule that interacts with the surface.⁹

Carbon monoxide has been often adopted to probe the structure of several metal oxide surfaces.^{9,10} In the case of TiO₂, the interaction of CO with the surface was observed to be reversible, with an adsorption energy in the order of 8–10 kcal/mol.^{11–13} The CO stretching frequency, equal to 2143 cm⁻¹ in the gas phase, shifts to higher wavenumbers upon adsorption on stoichiometric surfaces. This shift is

attributed to the polarization of the CO molecule under the electric field of the metal cation, which enhances the charge separation and strengthens the C–O bond.⁹ In an early spectroscopic analysis, Yates reported frequencies of 2182 and 2188 cm⁻¹ for the vibration of CO chemisorbed on rutile and anatase, respectively.¹⁴ Subsequent IR studies on both polymorphs of titania have shown comparable results, detecting the CO vibration somewhere in the range 2175–2210 cm⁻¹, depending on the sample, the surface coverage, and the experimental conditions.^{14–25} Occasionally, along with these bands additional peaks were observed 10–30 cm⁻¹ below the gas phase frequency, which have been assigned to carbonate species,¹⁵ “physically adsorbed” CO,¹⁹ or adsorption on reduced sites.^{16,21} It should be noted that, in most of these studies, a microscopic description of the surface was not available, implying little or no information on the identity and the relative abundance of the different exposed faces, the type, and the proportion of vacancies, etc. In this scenario, the adsorption sites have been classified with greek letters (e.g., α , β , β' , γ), according to the observed frequency, abundance, and the stability of the adsorbates.¹⁷ The assignment of each of these sites to a particular coordination and oxidation state of the Ti cation remained ambiguous in many cases.¹⁷ As far as we are aware, the recent FTIR experiments on single crystals by Wöll and co-workers, focused on rutile (110)^{22,23} and on anatase (101),²⁴ together with the infrared reflection-adsorption spectroscopy (IRAS) measurements by Petrik and Kimmel,²⁵ are the only studies to address well-defined TiO₂

^{a)}Authors to whom correspondence should be sent. Electronic mail: lustemberg@ifir-conicet.gov.ar and damian@qi.fcen.uba.ar

surfaces. These investigations have suggested that vacancies in reduced rutile (110) are responsible for a downshift in the CO stretching peak of around 10 cm^{-1} with respect to the frequency corresponding to the oxidized face.^{23,25} Also, some of these experiments on rutile (110) have suggested that in the high pressure regime, for coverages above 1 ML, a fraction of the CO molecules would adsorb parallel to the surface.²⁵

A number of electronic structure calculations has been performed for the interaction of CO with different models of the TiO_2 surface.^{26–39} Sorescu and Yates, in one of the first studies to consider periodic slabs, applied density functional theory (DFT) to characterize the adsorption geometry and energetics of carbon monoxide on the stoichiometric and defective rutile (110) surface at different coverages.^{28,29} The adsorption energy, estimated in 9 kcal/mol for the undefective rutile, was observed to decrease for monolayer coverage due to repulsive interactions. Similar results were found in later DFT studies on periodic slabs representing stoichiometric rutile and anatase surfaces,^{31,32,34–36,38,39} in some of which the stretching frequency of the CO mode was estimated through the harmonic approximation: a value of 2203 cm^{-1} was reported for anatase (101),³⁴ and between 2194 and 2207 cm^{-1} for rutile (110).^{34–36} For the reduced surface, information from electronic structure calculations is much scarcer. Adsorption energies of 7.4 and 36 kcal/mol were obtained by Sorescu and Yates on the rutile (110) surface in the presence of single and double oxygen vacancies, respectively.²⁹ In particular, for the case of a single vacancy coverage of 0.5, these authors found that CO adsorption is favored on the bridging-oxygen defect. A recent study combining scanning tunneling microscopy (STM) experiments with simulations on a larger supercell, however, indicated that at a low vacancy density the adsorption occurs most likely on five-coordinate titanium atoms, away from the vacancy sites.³⁷ Even more recently, Farnesi Camellone and co-workers examined this problem in a (4×2) rutile (110) supercell, using both DFT and DFT+U.³⁸ In reduced anatase and rutile slabs, pure DFT methods underestimate the electronic band gap and produce charge-delocalized solutions, in spite of the existing experimental results revealing localized electron states within the gap.⁴⁰ This problem can be addressed using DFT+U: in the presence of oxygen vacancies, inclusion of a Hubbard U term yields solutions with one or two electrons localized on Ti atoms. Kowalski and co-workers have shown via PBE+U molecular dynamics simulations of the reduced rutile slab that several localized electronic states can be characterized, lying very close in energy and separated from each other by low activation barriers.⁴¹ Each of these states exhibits a different distribution for the excess electrons, which may localize on surface or—most frequently—on subsurface Ti atoms. In spite of the disparate performances of DFT and DFT+U, however, the CO adsorption energetics on reduced rutile (110) were found to be little sensitive to the inclusion of the Hubbard U term.³⁸ The adsorption energy on the site identified as the most stable by experiments as well as pure DFT calculations³⁷ changes from 0.30 eV in PBE to 0.29 eV in PBE+U.³⁸ Accordingly, we expect only minor differences between the DFT and the DFT+U vibrational frequencies and, in any case, such differences should tend to disappear as the atoms involved are fur-

ther from the vacancy and from the excess charge. While the electronic structure picture is undoubtedly improved with the inclusion of the Hubbard U term, the results for CO suggest that this improvement does not directly translate into a correction of the adsorption energies on atoms residing some bonds away from the localized charge. In particular, these authors found that the CO adsorption energy does not vary significantly between the different Ti^{4+} sites of the reduced rutile (110) face, neither on the bridging oxygen vacancy, falling always in the range 7 ± 0.5 kcal/mol, with the exception of the Ti center next to the vacancy for which DFT+U yields a lower affinity.³⁸ On the other hand, to the best of our knowledge the interaction of CO with the reduced anatase surface has not been explored with computer simulations.

In spite of the numerous investigations on the effect of the surface structure on the frequency shift of the CO stretching mode, there is still not a general agreement on the assignment of the peaks, aside from those ascribed to the undefective, Ti^{4+} sites. In this article, we present calculations of the frequencies of the CO molecule adsorbed on different sites of defective and undefective anatase (101) and rutile (110) surfaces. These frequencies were computed from DFT and Car-Parrinello molecular dynamics simulations, via the Fourier transform of the time autocorrelation functions obtained from the molecular trajectories. In this way, we intend to provide a catalogue of the characteristic frequencies associated with each kind of site in the (110) and (101) faces. Our purpose is to shed some light on the adsorption energetics of CO on reduced TiO_2 and, more specifically, on the interpretation of FTIR data and the spectroscopic identification of defects in titania surfaces, which continues to be an ambiguous and controversial practice.

II. METHODOLOGY

A. Electronic structure calculations

All electronic structure calculations were performed using density functional theory in periodic boundary conditions as implemented in the Quantum-Espresso package.⁴² The Kohn-Sham orbitals and charge density were expanded in plane-waves basis sets up to a kinetic energy cutoff of 25 Ry and 200 Ry, respectively. The Perdew-Wang (PW91) approach to the exchange-correlation energy^{43,44} and Vanderbilt ultrasoft pseudopotentials⁴⁵ were adopted to compute the total energies and forces. Our preliminary tests on reduced slabs have shown that spin-polarized calculations converge to zero spin-density wavefunctions, in agreement with previous work,^{33,37} therefore all reported computations have been conducted in the spin-restricted framework. Geometry optimizations were performed at the Born-Oppenheimer approximation, while molecular dynamics simulations were carried out within the Car-Parrinello method⁴⁶ using a N ose Hoover thermostat at 150 K and a time step of 0.19 fs. In the calculation of geometries and adsorption energies, Monkhorst-Pack grids of sizes $3 \times 3 \times 1$ and $3 \times 2 \times 1$ were used for reciprocal space sampling in rutile and anatase slabs, respectively. In the molecular dynamics simulations, calculations were restricted to the Γ -point.

B. Model systems

The anatase (101) surface was represented by a (2×2) supercell, whereas in the case of rutile (110), a (2×1) surface was adopted. The supercell dimensions were $7.55 \times 10.24 \times 18.9 \text{ \AA}^3$ for anatase and $6.01 \times 6.48 \times 27.04 \text{ \AA}^3$ for rutile, both of them consisting of six layers in the z -direction, containing a total of 72 atoms in the absence of vacancies. Calculations for the (110) rutile surface were also performed in a (4×2) supercell with four and three layers (192 and 144 atoms) to examine the role of vacancy concentration in the CO binding.

C. IR absorption lineshapes

The vibrational frequency of the CO molecule was computed from the Fourier transform of the time correlation function of the atomic velocities, $\mathbf{v}(t)$:⁴⁷

$$I(\omega) = \frac{1}{2\pi} \int_{-\infty}^{\infty} dt e^{-i\omega t} \langle \mathbf{v}(0) \mathbf{v}(t) \rangle. \quad (1)$$

Different implementations of this approach have been employed to calculate the IR adsorption spectra of water in various environments, namely in bulk,⁴⁸ confined,⁴⁹ and interfacial.⁵⁰ To construct the time autocorrelation functions, positions and velocities were collected every 0.97 fs along time windows of at least 5 ps. Depending on the system and on the electronic-mass, ionic frequencies in Car-Parrinello dynamics may present typical downshifts of 4%–8% with respect to spectroscopic data.⁵¹ In the particular case of CO, an underestimation of 103 cm^{-1} has been informed for the local density approximation (LDA) exchange correlation functional.⁵² Our computations based on the PW91 functional show exactly the same downshift with respect to the experimental frequency. Therefore, we have applied a correction of 103 cm^{-1} to our reported values, to make comparison with experiments straightforward. This is properly indicated in all figures and tables.

III. RESULTS AND DISCUSSION

A. Undefective surfaces

As reported in previous studies of CO on the TiO_2 rutile (110) face,^{28–32,34} DFT predicts a vertical adsorption geometry, with the carbon atom pointing towards the surface. Our simulations in a (2×1) unit cell of rutile (110) yield a Ti–C distance of 2.50 \AA and an adsorption energy of 6.55 kcal/mol . These values are in reasonable agreement with the available experimental data and with previous calculations in the same model slab. Calculations on a larger model of the rutile face, a (4×2) supercell with a CO coverage 8 times lower, provide an adsorption energy about 1 kcal/mol higher than in the (2×1) slab, probably due to the minimization of repulsive lateral interactions between CO molecules.

In the case of the anatase (101) surface, the Ti–C bond length and adsorption energy turn out to be, respectively, 2.51 \AA and 6.95 kcal/mol . To the best of our knowledge, there are two groups who have examined the behavior of CO on TiO_2 anatase applying electronic structure calcu-

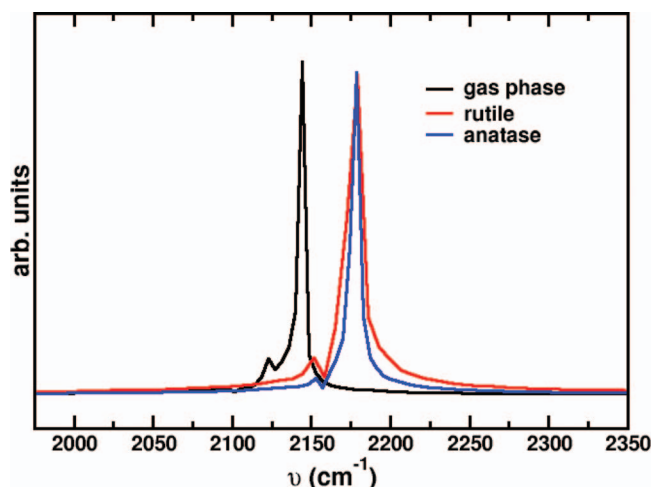


FIG. 1. Simulated IR spectra of the CO molecule on the stoichiometric (110) and (101) surfaces of TiO_2 rutile and anatase, respectively. The peak obtained for the free CO molecule is also shown. A correction of 103 cm^{-1} has been applied to the data (see text).

lations. Wanbayer and co-workers found adsorption energies falling between 6 and 6.78 kcal/mol , depending on the methodology.^{39,53} On the other hand, Scaranto and Giorgianni reported for the bond length and the adsorption energy, values of 2.44 \AA and 4.15 kcal/mol ,³⁴ respectively, based on B3LYP calculations with Gaussian basis sets. About the same adsorption energy was informed in this study for the rutile (110) face, which turns out to be significantly lower than the experimental values or the values obtained using plane-waves basis and pure DFT functionals.

Despite a difference of 6% between the CO adsorption energies on rutile and anatase, the effect of both surfaces on the frequency of the vibrational mode seems to be practically the same. According to our simulations, anatase and rutile cause blueshifts of 35 and 36 cm^{-1} in the stretching frequency. If the correction of 103 cm^{-1} is applied, the predicted IR frequencies are 2178 and 2179 cm^{-1} for anatase and rutile, respectively. The simulated bands are overlapping in Figure 1, which illustrates the peaks of CO adsorbed on the stoichiometric (101) and (110) surfaces, along with the gas phase band. It should be noticed that the (2×1) slab model of rutile (110) represents a surface coverage of 0.5 ML. Simulations on the (4×2) supercell representing a CO coverage of 0.0625 ML, give for the carbon monoxide vibration a signal at 2188 cm^{-1} , suggesting that the absorption band moves to higher wavenumbers with decreasing pressure (Table I). In the (110) face of rutile single crystals, the measured CO frequency was 2183 cm^{-1} at 110 K and 10^{-7} mbar .²² Upon evacuation, and as a consequence of a drop in surface coverage, this peak decreases in intensity and shifts to higher values, reaching 2190 cm^{-1} for 10^{-10} mbar , in excellent agreement with our results. On the other hand, the CO stretching on anatase (101) has been characterized at 2180 cm^{-1} ,²⁴ also in line with our computations.

B. The defective rutile (110) surface

The incidence of reduced TiO_2 surfaces on the CO vibration frequency is still a matter of discussion. It has been

TABLE I. Calculated adsorption energies, optimized distances, and frequency for CO on the undefective and defective (110) surface of rutile TiO_2 . $\Delta\nu$ indicates the frequency shift with respect to the free CO molecule. The reported frequency ν includes a correction of 103 cm^{-1} , applied to the Car-Parrinello result (see text). BOv refers to adsorption on the bridging oxygen vacancy.

Surface type/configuration	Rutile				
	E_{ADS} (kcal/mol)	Ti-C (Å)	C-O (Å)	$\Delta\nu$ (cm^{-1})	ν (cm^{-1}) ^a
Undefective ^b	6.55	2.50	1.138	+36	2179
One vacancy/BOv ^b	10.5	2.37/3.03	1.142	−158	1985
One vacancy/site 0 ^b	4.07	2.57	1.139	−5	2138
One vacancy/site 1 ^b	6.61	2.44	1.139	−45	2098
Two vacancies ^b	43.7	1.99/2.16	1.219	−505	1638
Undefective ^c	7.78	2.45	1.137	+45	2188
One vacancy/BOv ^c	7.01	2.82/2.87	1.138
One vacancy/site 0 ^c	6.33	2.46	1.137
One vacancy/site 1 ^c	7.54	2.43	1.137	+37	2180

^aCorrected according to the Car-Parrinello deviation.

^b(2×1) unit cell.

^c(4×2) unit cell.

argued that adsorption on Ti^{3+} sites leads to redshifts which vary from 10 to 30 cm^{-1} ,^{16,21} while other researchers support the idea that such a peak cannot be observed because Ti^{3+} centers react with CO provoking the oxidation of the surface.¹⁷ This controversy has been seemingly resolved, at least for the case of the rutile (110) face in high vacuum, since a recent study combining STM measurements with plane-waves DFT calculations.³⁷ In this work a (6×2) unit cell including a bridging-oxygen vacancy was employed; this model is much larger than the supercells generally examined in previous simulations. Calculations on this large slab revealed that the most favored site for CO adsorption was not on the vicinity of the oxygen vacancy, but on a five-coordinate Ti atom separated from the defect by two bonds. This titanium atom is marked as site 1 in Figure 2, following the notation introduced in Ref. 37, which we will adopt hereafter. Moreover, the carbon monoxide adsorption energies were comparable (about 8.8 kcal/mol) on any five-coordinate titanium atom located farther from the vacancy. On the closest Ti^{4+} atom (site 0) the interaction turned out to be of 7.4 kcal/mol and on top of the oxygen vacancy of only 3.8 kcal/mol.³⁷ These findings were consistent with the STM data presented in the same study, but at variance with previous calculations using a (2×1) unit cell,²⁹ predicting that adsorption would occur on the oxygen defect for a vacancy coverage of 0.5. The adsorption energies calculated in the smaller slab were 7.4 and 4.7 kcal/mol on the vacancy and on site 0, respectively. Our own simulations in the (2×1) system show agreement with these results (see Table I). The vibrational frequency for the CO adsorbed on this defective surface, according to our time correlation function analysis, should be 1985 cm^{-1} . Yet, this situation corresponds to a surface-vacancy concentration of 0.5, which is much higher than the one usually present in reduced samples.

Interestingly, these results indicate that the adsorption site is strongly dependent on vacancy concentration. The inversion in the relative CO affinity between the five-coordinate (Ti^{4+}) and the vacancy (Ti^{3+}) sites in going from the small to the large slab can be rationalized recalling that the bond between the molecule and the Ti^{4+} site is to a great extent an electrostatic interaction. The excess charge in Ti^{3+} reinforces

the σ -bond and allows for some backbonding from the d electrons of the cation to the antibonding orbitals of the CO.¹⁰ This leads to a partial occupation of the π -antibonding orbital of CO, which weakens the carbon-oxygen bond while the metal-carbon bond is strengthened. In the Ti^{4+} site this effect is almost negligible and the bond is essentially electrostatic.¹⁰ Moreover, in the case of a low vacancy density, as in the (6×2) or (4×2) unit cells, the excess charge is quite delocalized over the adjacent Ti cations,⁵⁴ the titanium atom next to the oxygen vacancy has an intermediate character between Ti^{3+} and Ti^{4+} , and the electrostatic interaction with the more positive five-coordinate cations prevails. As the concentration of vacancies is increased, the delocalization of the excess charge becomes more restrained and therefore the formal oxidation state of the undercoordinate Ti atoms becomes closer to 3+. This interpretation is further supported by the analysis of the charge transfer from the surface to the molecule, estimated from the projected density of states (PDOS) on the CO orbitals, which is depicted in Figure 3. It can be seen that when the CO adsorbs on a vacancy, the integrated PDOS yields a larger population if the vacancy density is higher, in the (2×1) slab, in comparison with the (4×2) cell. In particular, the CO integrated charge in the former slab turns out to be $0.17e$ larger, reflecting the excess charge transferred from the surface to the adsorbate.

For low bridging-oxygen vacancy concentrations—less than 22% according to Ref. 37—the carbon monoxide molecule will be predominantly adsorbed on a five-coordinated titanium atom (site 1). Therefore, it will be of interest to determine the vibrational shift of CO bound to this site, in particular to query whether it could be used as a reporter on the presence of a nearby oxygen vacancy. Two independent, very recent IR studies on reduced rutile (110) surfaces, have identified a pair of peaks appearing at approximately 2178 and 2188 cm^{-1} .^{23,25} On the basis of comparisons with the oxidized surface, on the effect of CO dosage, and on auxiliary static DFT calculations, the band at 2178 cm^{-1} was assigned to CO bound to Ti cations located in the vicinity of an oxygen vacancy (i.e., on site 1), while the band at 2188 cm^{-1} was attributed to CO adsorbed on perfect parts

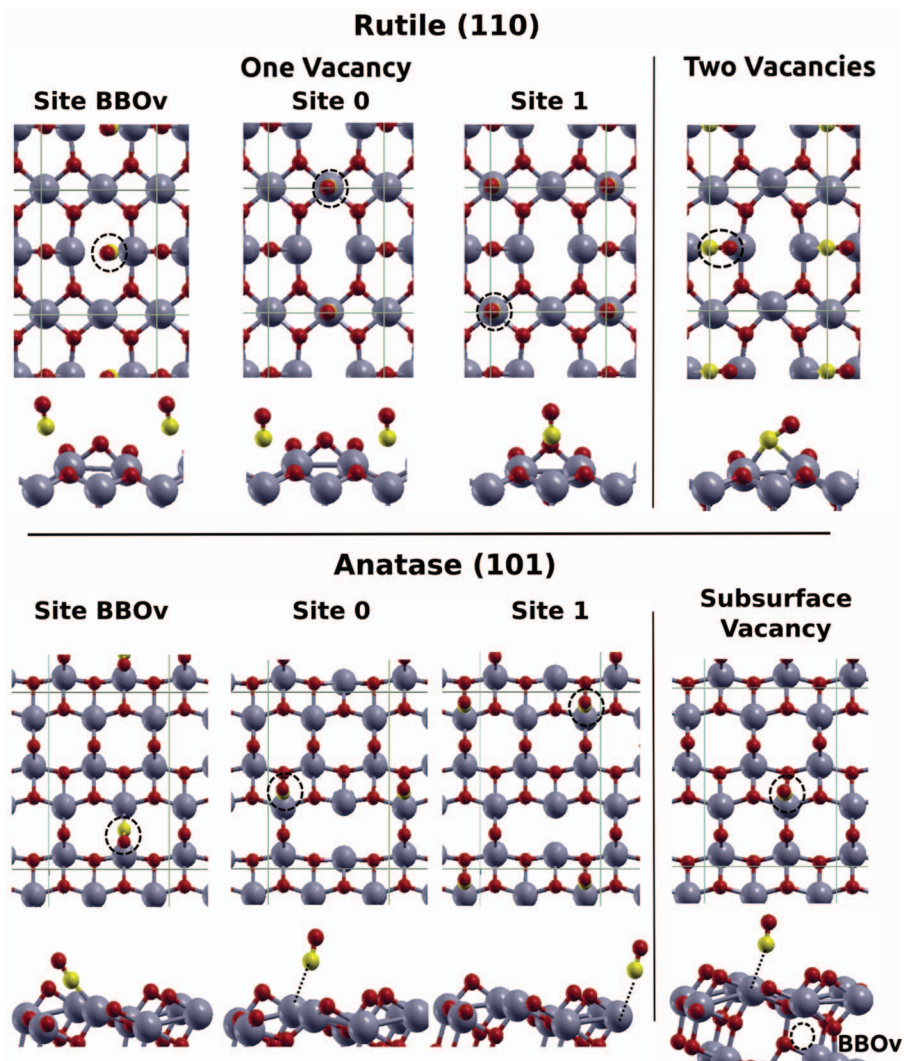


FIG. 2. Top and side views of the optimized, reduced TiO_2 surface models, including the adsorbed CO on the different sites examined. Ti, O, and C atoms are depicted in blue, red, and yellow, respectively. The dashed circles mark the position of the CO molecule (top views) and of the subsurface oxygen vacancy (side view). Ov stands for oxygen vacancy.

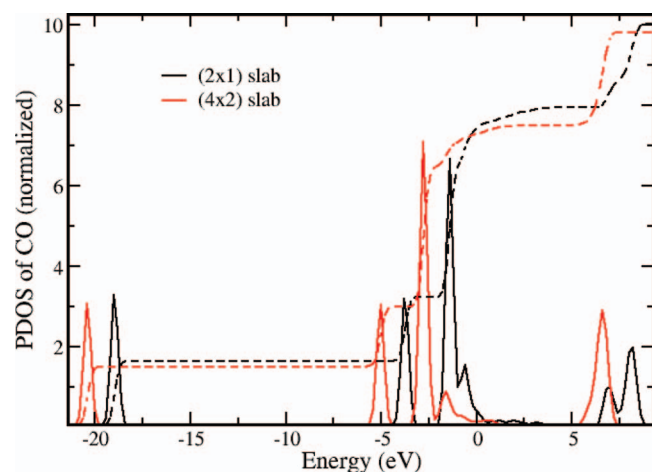


FIG. 3. Density of states projected on the atomic orbitals of the CO molecule adsorbed at the bridging-oxygen site, in the (4×2) and (2×1) model slabs of the rutile (110) surface. The dashed lines show the integration of the projected density of states. The smaller charge integrated for the (4×2) -cell reflects a higher delocalization of the electronic density around the defect, with respect to the (2×1) -cell.

of the surface. The realization of DFT molecular dynamics simulations on the (6×2) unit cell to extract this information would be exceedingly costly. Because of this, we have examined the vibrational shift in a slightly smaller system, a (4×2) slab containing three TiO_2 layers, which, while being computationally more affordable, still captures the inversion in the relative affinity between site 1 and the oxygen vacancy observed in the bigger unit cell. Table I shows the adsorption energies on different sites of the (4×2) slab: it is seen that the interaction results slightly larger on the five-coordinate titanium centers (save site 0) if compared to the vacancy site. Thus, the energetics in this unit cell is in between the case of the (2×1) model, where the interaction on the vacancy is favored by 4 kcal/mol with respect to the perfect surface, and the case of the (6×2) model, where the adsorption on the vacancy is unfavored by 5 kcal/mol.³⁷ More important, the vibrational frequency on site 1 (2180 cm^{-1}) is red-shifted in 8 cm^{-1} with respect to the value obtained on the undefective surface in the same unit cell (2188 cm^{-1}). This result is in full agreement with the experimental data, supporting the

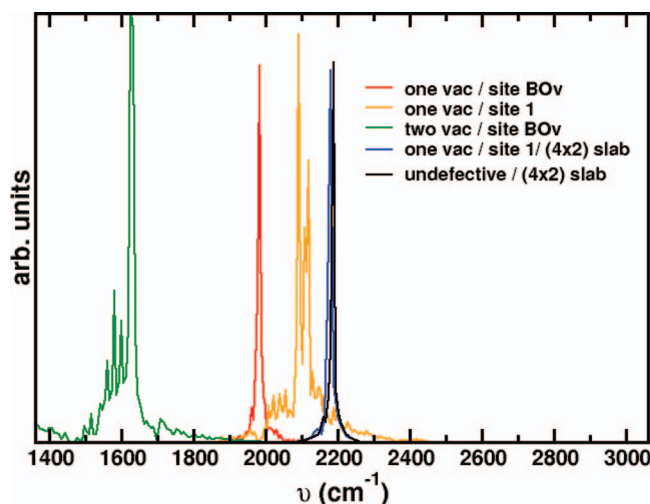


FIG. 4. Simulated IR spectra of the CO molecule on the stoichiometric and defective (110) surfaces of TiO_2 rutile, with single and double vacancies. The different adsorption sites are displayed in Figure 2. BOv stands for bridging oxygen vacancy. A correction of 103 cm^{-1} has been applied to the data (see text).

proposal that CO spectroscopy can be used to quantify the oxygen vacancy concentration on rutile (110) samples, as discussed in Ref. 23.

Finally, the possibility of adsorption on a double vacancy originating in the absence of two adjacent bridging-oxygen atoms was explored in the (2×1) unit cell. As previously reported by Sorescu and Yates,²⁹ the CO molecule tightly binds to this kind of defect: our DFT calculations show that the CO adsorbs in an angular geometry, with the C atom occupying the position of the bridging-oxygen, and the O atom tilted toward one of the neighboring four-coordinate Ti cations (Figure 2), yielding an interaction energy of 43.7 kcal/mol. The vibrational C–O mode is hence strongly perturbed, giving rise to a split peak at around 1638 cm^{-1} (Figure 4). Therefore it should be possible to identify this kind of defects in high vacuum based on the spectroscopy of the CO molecule. Signals in this region that could be ascribed to this mode have been occasionally reported in rutile samples.¹⁹

C. The defective anatase (101) surface

At variance with the case of rutile (110), the CO molecule has a strong affinity towards single oxygen vacancies on the anatase (101) surface. A bridging-oxygen vacancy leaves a four-coordinate titanium atom on the anatase surface, which interacts with CO. Table II shows that this interaction is several times larger than any other involving the five-coordinate titanium atoms located around the defective site. The adsorption geometry is depicted in Figure 2. Here, we do not expect a significant effect due to system size, as in the case of rutile, since the adsorption energy on a titanium atom placed two bonds away from the vacancy—which we denote as site 2—reaches practically the same value as in the undefective surface (it should be noticed that the anatase supercell used here has twice the number of surface atoms than the rutile (2×1) supercell).

TABLE II. Calculated adsorption energies, optimized distances, and frequency for CO on the undefective and defective (101) surface of anatase TiO_2 . $\Delta\nu$ indicates the frequency shift with respect to the free CO molecule. The reported frequency ν includes a correction of 103 cm^{-1} , applied to the Car-Parrinello result (see text). BOv refers to adsorption on the bridging oxygen vacancy.

Surface type/ configuration	Anatase				
	E_{ADS} (kcal/mol)	Ti–C (Å)	C–O (Å)	$\Delta\nu$ (cm^{-1})	ν (cm^{-1}) ^a
Undefective	6.95	2.51	1.138	+35	2178
One vacancy/BOv	22.2	2.09	1.169	−207	1936
One vacancy/site 0	6.69	2.50	1.138
One vacancy/site 1	6.35	2.42	1.139	−15	2128
Subsurface	7.25	2.46	1.138	−20	2123

^aCorrected according to the Car-Parrinello deviation.

According to our simulations, the interaction with the defective anatase surface should cause a vibrational redshift of around 207 cm^{-1} in the CO stretching (Table II and Figure 5). However, and to the best of our knowledge, experimental spectra of CO on reduced TiO_2 samples do not exhibit any characteristic band in the region of 1930 cm^{-1} that can be ascribed to such a mode. A possible reason for the absence of this signal could be the low exposition of oxygen vacancies on the anatase (101) surface. Recent STM experiments⁵⁵ and DFT calculations^{56,57} have shown that, at variance with the case of rutile (110), oxygen vacancies on the (101) face of anatase are more stable (by around 0.5 eV) at subsurface positions than at the surface. Moreover, the diffusion barrier is low enough for a defect to migrate spontaneously to the bulk if a vacancy is created on the surface by sputtering or annealing techniques.^{56,57} The remotion of a bridging oxygen atom leaves behind two five-coordinate titanium atoms in the rutile (110) face; instead, it leaves a five-coordinate and a four-coordinate titanium atom on the anatase (101) surface,

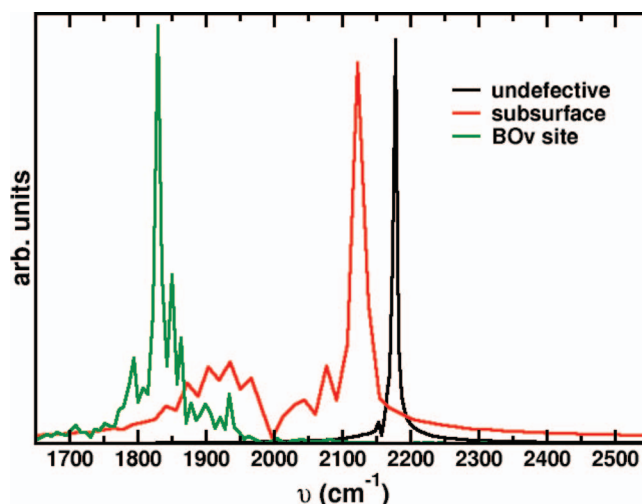


FIG. 5. Simulated IR spectra of the CO molecule on the stoichiometric and defective (101) surfaces of TiO_2 anatase, with surface and subsurface oxygen vacancies. The corresponding adsorption sites are displayed in Figure 2. BOv stands for bridging oxygen vacancy. A correction of 103 cm^{-1} has been applied to the data (see text).

entailing a higher formation energy for the defect in comparison to the former. According to these results, subsurface oxygen vacancies would predominate over surface vacancies in anatase (101),^{55–57} whereas the opposite will be true in rutile (110).⁵⁷

Based on these findings, we have explored the effect of a subsurface vacancy on the frequency of a CO molecule adsorbed in the vicinity of the defect. In particular, in our model the O-vacancy resides in the second TiO₂ layer, immediately below the surface, reproducing one of the most stable structures found using DFT.⁵⁷ Figure 2 depicts the structure of the adsorbate relaxed on this defective anatase slab. The CO adsorption energy on the five coordinate titanium atom lying above the vacancy is around 0.3 kcal/mol higher than on five coordinate Ti atoms of the undefective surface (Table II). Assuming a Boltzmann distribution at 150 K and an equal availability of defective and non-defective sites, this means that titanium atoms above subsurface defects will be about three times more populated with carbon monoxide. Moreover, this adsorption mode causes a downshift of 20 cm^{−1} in the CO stretching frequency (Table II). The combination of these two circumstances—a favored binding and a significant displacement of the CO signal—provides a worthy resource for quantitative determination of oxygen-vacancies in TiO₂ anatase. Interestingly, bands in the region 2110–2130 cm^{−1} have been often informed in IR spectra of CO on anatase, whose assignment has been generally ambiguous and a matter of discussion in the literature (see, for example, Refs. 15, 16, and 21). It may be also worth noticing that, regardless of the surface or subsurface nature of the defect, the shift in the CO vibrational frequency for the adsorption on a defect second-neighbor is always similar (−15 cm^{−1} versus −20 cm^{−1}, see entries corresponding to “Site 1” and “Subsurface” in Table II). This reflects that the electronic structure at the Ti⁴⁺ site is affected to a comparable extent by the charge delocalization arising from a missing oxygen atom from the surface or from the bulk.

In brief, our results suggest that reduced anatase samples should exhibit a peak at around 2123 cm^{−1} originating in the CO bound on five-coordinate titanium atoms lying above subsurface vacancies, whose intensity would be indicative of the degree of reduction.

IV. SUMMARY AND CONCLUSIONS

We have investigated the energetics and the stretching frequencies for the adsorption of carbon monoxide on perfect and defective faces of titanium dioxide, using Car-Parrinello molecular dynamics. We observed a vibrational shift of ≈35–45 cm^{−1} on stoichiometric TiO₂ surfaces, depending on surface coverage; this shift is approximately the same on both rutile (110) and anatase (101) faces, despite a difference of about 6% in the corresponding adsorption energies. In reduced rutile (110), the predominant adsorption site is strongly dependent on vacancy concentration. In the low density limit, the most stable adsorption takes place on five coordinate titanium atoms located at least two bonds away from the vacancy. The vibrational frequency of CO absorbed on Ti atoms adjacent to oxygen vacancies is around 10 cm^{−1} below the value obtained in the undefective surface, so that with current ex-

perimental spectral resolution it should be feasible to tell one from the other. As the concentration of vacancies increases, the adsorption on the defect becomes thermodynamically favored. The Ti³⁺ cations turn out to be the most stable adsorption sites when the vacancy coverage is 0.5. This behavior can be understood as an interplay between covalent and electrostatic binding: the higher electron density available on Ti³⁺ contributes to the σ -bond and possibly allows for some Π back-donation from the metal to the molecule. In an isolated vacancy the charge density is substantially more delocalized, which impairs the covalent binding and then the electrostatic interaction with Ti⁴⁺ sites dominates. In the presence of double-vacancies, the CO molecule becomes tightly bound to four coordinate titanium atoms, the CO frequency experiencing a strong downshift.

On the anatase (101) surface, Ti³⁺ sites are the ones exhibiting the highest affinity for CO, causing a downshift in the bond stretching of 207 cm^{−1} with respect to the free molecule. No band at this position that can be assigned to such a mode, however, has been reported in experiments as far as we are aware. We attribute this fact to the low concentration of surface vacancies present in anatase (101), for which it has been recently shown that subsurface vacancies must predominate.^{55–57} We found that, in the presence of subsurface oxygen defects, CO adsorption is driven toward the five coordinate Ti atoms residing on top of the vacancies. This mode causes a redshift of 20 cm^{−1} in the vibrational frequency of the adsorbate, which should make it feasible the quantitative identification of subsurface vacancies in TiO₂ anatase. Moreover, this result settles the assignment of a band typically present in the IR spectra of CO on TiO₂, whose origin has been the subject of controversy in the experimental literature.^{15,16,19,21}

ACKNOWLEDGMENTS

We thank Dr. Nano Gonzalez Lebrero for technical advice and valuable discussions. We are also grateful to the referees, who have provided a constructive critical review and have pointed out essential recent literature. This work was supported by funding granted to D.A.S. by ANPCYT (Grant No. PICT07-2111). We acknowledge time allocation in the supercomputer Cristina, funded by ANPCYT, Grant No. PME-2006-01581, and the HPC cluster Rosario, both adherents to the National System for High Performance Computing (SNCAD).

¹U. Diebold, *Surf. Sci. Rep.* **48**, 53 (2003).

²X. Chen and S. S. Mao, *Chem. Rev.* **107**, 2891 (2007).

³M. A. Henderson, *Surf. Sci. Rep.* **66**, 185 (2011).

⁴S. Bajt, N. Edwards, and T. E. Madey, *Surf. Sci. Rep.* **63**, 73 (2008).

⁵B. O'Regan and M. Grätzel, *Nature (London)* **353**, 737 (1991).

⁶S. Yanagida, Y. Yu, and K. Manseki, *Acc. Chem. Res.* **42**, 1827 (2009).

⁷Y. Lin, Y. Li, and X. Zhan, *Chem. Soc. Rev.* **41**, 4245 (2012).

⁸C. Sanchez, P. Belleville, M. Popall, and L. Nicole, *Chem. Soc. Rev.* **40**, 696 (2011).

⁹C. Lamberti, A. Zecchina, E. Groppo, and S. Bordiga, *Chem. Soc. Rev.* **39**, 4951 (2010).

¹⁰K. I. Hadjiivanov and G. N. Vayssilov, *Adv. Catal.* **47**, 307 (2002).

¹¹G. B. Raupp and J. A. Dumesic, *J. Phys. Chem.* **89**, 5240 (1985).

¹²A. Linsebigler, G. Lu, and J. T. Yates, *J. Chem. Phys.* **103**, 9438 (1995).

- ¹³Z. Dohnálek, J. Kim, O. Bondarchuk, J. M. White, and B. D. Kay, *J. Phys. Chem. B* **110**, 6229 (2006).
- ¹⁴D. J. C. Yates, *J. Phys. Chem.* **65**, 746 (1961).
- ¹⁵K. Tanaka and J. M. White, *J. Phys. Chem.* **86**, 4708 (1982).
- ¹⁶G. Busca, H. Saussey, O. Saur, J. C. Lavalley, and V. Lorenzelli, *Appl. Catal.* **14**, 245 (1985).
- ¹⁷K. I. Hadjiivanov and D. G. Klissurski, *Chem. Soc. Rev.* **25**, 61 (1996).
- ¹⁸K. Hadjiivanov, J. Lamotte, and J.-C. Lavalley, *Langmuir* **13**, 3374 (1997).
- ¹⁹K. Hadjiivanov, *Appl. Surf. Sci.* **135**, 331 (1998).
- ²⁰G. Busca, *Catal. Today* **41**, 191 (1998).
- ²¹L. F. Liao, C. F. Lien, D. L. Shieh, M. T. Chen, and J. L. Lin, *J. Phys. Chem. B* **106**, 11240 (2002).
- ²²C. Rohmann, Y. Wang, M. Muhler, J. B. Metson, H. Idriss, and C. Wöll, *Chem. Phys. Lett.* **460**, 10 (2008).
- ²³M. Xu, H. Noei, K. Fink, M. Muhler, Y. Wang, and C. Wöll, *Angew. Chem., Int. Ed.* **51**, 4731 (2012).
- ²⁴M. Xu, Y. Gao, E. M. Moreno, M. Kunst, M. Muhler, Y. Wang, H. Idriss, and C. Wöll, *Phys. Rev. Lett.* **106**, 138302 (2011).
- ²⁵N. G. Petrik and G. A. Kimmel, *J. Phys. Chem. Lett.* **3**, 3425 (2012).
- ²⁶G. Pacchioni, A. M. Ferrari, and P. S. Bagus, *Surf. Sci.* **350**, 159 (1996).
- ²⁷M. Casarin, C. Maccato, and A. Vittadini, *J. Phys. Chem. B* **102**, 10745 (1998).
- ²⁸D. C. Sorescu and J. T. Yates, Jr., *J. Phys. Chem. B* **102**, 4556 (1998).
- ²⁹D. C. Sorescu and J. T. Yates, Jr., *J. Phys. Chem. B* **106**, 6184 (2002).
- ³⁰Z. Yang, R. Wu, Q. Zhang, and D. W. Goodman, *Phys. Rev. B* **63**, 045419 (2001).
- ³¹M. Menetrey, A. Markovits, and C. Minot, *Surf. Sci.* **524**, 49 (2003).
- ³²X. Wu, A. Selloni, and S. K. Nayak, *J. Chem. Phys.* **120**, 4512 (2004).
- ³³D. Pillay and G. S. Hwanga, *J. Chem. Phys.* **125**, 144706 (2006).
- ³⁴J. Scaranto and S. Giorgianni, *J. Mol. Struct.: THEOCHEM* **858**, 72 (2008).
- ³⁵J. Scaranto and S. Giorgianni, *Chem. Phys. Lett.* **473**, 179 (2009).
- ³⁶M. Kunat, F. Traeger, D. Silber, H. Qiu, Y. Wang, A. C. van Veen, C. Wöll, P. M. Kowalski, B. Meyer, C. Hätting *et al.*, *J. Chem. Phys.* **130**, 144703 (2009).
- ³⁷Y. Zhao, Z. Wang, X. Cui, T. Huang, B. Wang, Y. Luo, J. Yang, and J. Hou, *J. Am. Chem. Soc.* **131**, 7958 (2009).
- ³⁸M. Farnesi Camellone, P. M. Kowalski, and D. Marx, *Phys. Rev. B* **84**, 035413 (2011).
- ³⁹R. Wanbayor, P. Deák, T. Frauenheim, and V. Ruangpornvisuti, *J. Chem. Phys.* **134**, 104701 (2011).
- ⁴⁰M. V. Ganduglia-Pirovano, A. Hofmann, and J. Sauer, *Surf. Sci. Rep.* **62**, 219 (2007).
- ⁴¹P. M. Kowalski, M. Farnesi Camellone, N. N. Nair, B. Meyer, and D. Marx, *Phys. Rev. Lett.* **105**, 146405 (2010).
- ⁴²P. Giannozzi *et al.*, *J. Phys. Condens. Matter* **21**, 395502 (2009), see <http://www.quantum-espresso.org/>.
- ⁴³J. P. Perdew and Y. Wang, *Phys. Rev. B* **45**, 13244 (1992).
- ⁴⁴J. P. Perdew *et al.*, *Phys. Rev. B* **46**, 6671 (1992).
- ⁴⁵D. Vanderbilt, *Phys. Rev. B* **41**, 7892 (1990).
- ⁴⁶R. Car and M. Parrinello, *Phys. Rev. Lett.* **55**, 2471 (1985).
- ⁴⁷D. A. McQuarrie, *Statistical Mechanics* (University Science Books, Sausalito, California, 2000).
- ⁴⁸P. L. Silvestrelli, M. Bernasconi, and M. Parrinello, *Chem. Phys. Lett.* **277**, 478 (1997).
- ⁴⁹F.-X. Coudert, R. Vuilleumier, and A. Boutin, *ChemPhysChem* **7**, 2464 (2006).
- ⁵⁰N. Kumar, S. Neogi, P. R. C. Kent, A. V. Bandura, J. D. Kubicki, D. J. Wesolowski, D. Cole, and J. O. Sofo, *J. Phys. Chem. C* **113**, 13732 (2009).
- ⁵¹P. Tangney and S. Scandolo, *J. Chem. Phys.* **116**, 14 (2002).
- ⁵²V. Wathelot, B. Champagne, D. H. Mosley, J.-M. André, and S. Massidda, *Chem. Phys. Lett.* **275**, 506 (1997).
- ⁵³R. Wanbayor and V. Ruangpornvisuti, *Mater. Chem. Phys.* **124**, 720 (2010).
- ⁵⁴T. Minato, Y. Sainoo, Y. Kim, H. S. Kato, K. ichi Aika, M. Kawai, J. Zhao, H. Petek, T. Huang, W. He *et al.*, *J. Chem. Phys.* **130**, 124502 (2009).
- ⁵⁵Y. He, O. Dulub, H. Cheng, A. Selloni, and U. Diebold, *Phys. Rev. Lett.* **102**, 106105 (2009).
- ⁵⁶H. Cheng and A. Selloni, *J. Chem. Phys.* **131**, 054703 (2009).
- ⁵⁷H. Cheng and A. Selloni, *Phys. Rev. B* **79**, 092101 (2009).